PHYSICAL REVIEW A, VOLUME 61, 051603(R)

Dissipation and vortex creation in Bose-Einstein condensed gases

B. Jackson,[1] J. F. McCann,[2] and C. S. Adams[1]
[1]*Department of Physics, Rochester Building, University of Durham, South Road, Durham, DH1 3LE, United Kingdom*
[2]*Department of Applied Mathematics and Theoretical Physics, Queen's University, Belfast, BT7 1NN, United Kingdom*
(Received 20 December 1999; published 5 April 2000)

We solve the Gross-Pitaevskii equation to study energy transfer from an oscillating ''object'' to a trapped Bose-Einstein condensate. Two regimes are found: for object velocities below a critical value, energy is transferred by excitation of phonons at the motion extrema; while above the critical velocity, energy transfer is via vortex formation. The second regime corresponds to significantly enhanced heating, in agreement with a recent experiment.

PACS number(s): 03.75.Fi, 67.40.Vs, 67.57.De

The existence of a critical velocity for dissipation is central to the issue of superfluidity in quantum fluids. The concept was first introduced by Landau in his famous criterion [1], where elementary excitations are produced above a velocity v_L. In liquid ^{4}He this process refers to the excitation of rotons, with $v_L \simeq 58$ ms^{-1}. However, much smaller critical values are observed experimentally, which prompted Feynman to propose that quantized vortices may be responsible [2].

Vortex nucleation in superfluid ^{4}He is difficult to explain quantatively. Strong interactions within the liquid, plus thermal and quantum fluctuations, impede formulation of a satisfactory microscopic theory. In contrast, Bose-Einstein condensation (BEC) in trapped alkali-metal gases [3,4] provides a relatively simple system for exploring superfluidity. Weakly interacting condensates can be produced with a negligibly small noncondensed component. This allows an accurate description by a nonlinear Schrödinger equation, often known as the Gross-Pitaevskii (GP) equation. The system also offers excellent control over the temperature, number of atoms, and interaction strength, as well as allowing manipulation of the condensate using magnetic and optical forces [3].

Recent experiments have produced vortices by coherent excitation [5] and cooling of a rotating cloud [6]. The existence of vortices was also inferred by Raman *et al.* [7], where a condensate was probed by an oscillating laser beam blue detuned far from atomic resonance. The optical dipole force expels atoms from the region of highest intensity, resulting in a repulsive potential. Although vortices were not directly imaged, significant heating of the cloud was observed only above a critical velocity, indicating a transition to a dissipative regime. This heating was found to depend upon the existence of a condensate, indicating that it must be due to the production of elementary excitations that subsequently populate the noncondensed fraction.

Critical velocities for vortex formation in superflow past an obstacle have been studied numerically by solution of the GP equation in a homogeneous condensate [8–10]. Simulations have also confirmed that vortices are nucleated when a laser beam is translated inside a trapped Bose condensed gas [11,12]. In this paper, we attempt to clarify the role of vortices in the experiment of Raman *et al.* [7] by presenting two-dimensional (2D) and three-dimensional (3D) simulations of an oscillating repulsive potential in a condensate. The motion transfers energy to the condensate, and we observe that the transfer rate increases significantly above the critical velocity for vortex formation.

Our simulations employ the GP equation for the condensate wave function $\Psi(\boldsymbol{r},\mathrm{t})$ in a harmonic trap $V_{\mathrm{trap}}(\boldsymbol{r}) = (m/2)\Sigma_j \omega_j^2 j^2$, $j=x,y,z$. For convenience, we scale in harmonic oscillator units (h.o.u.), where the units of length, time, and energy are $(\hbar/2m\omega_x)^{1/2}$, ω_x^{-1}, and $\hbar\omega_x$, respectively. The scaled GP equation is then

$$i\partial_t \Psi = (-\nabla^2 + V + C|\Psi|^2)\Psi, \tag{1}$$

where V represents a time-dependent ''object'' potential superimposed upon a stationary trap: $V = \frac{1}{4}(x^2 + \epsilon y^2 + \eta z^2) + V_{\mathrm{ob}}(\boldsymbol{r},\mathrm{t})$. The atomic interactions are parametrized by $C = (NU_0/\hbar\omega_x)(2m\omega_x/\hbar)^{\gamma/2}$: N atoms of mass m interact with a s-wave scattering length a, such that $U_0 = 4\pi\hbar^2 a/m$. The number of dimensions is γ. For most of the simulations here, $\gamma = 2$, corresponding to the limit $\eta \to 0$. In this case, N represents the number of atoms per unit length along z. For the general 3D situation, a moving laser beam focused to a waist $\tilde{w}_0$ (in h.o.u.) at $(0,y'(t),0)$, is simulated using

$$V_{\mathrm{ob}}(\mathbf{r},\mathrm{t}) = \frac{U_{\mathrm{ob}}}{\sigma}\exp\left[\frac{-2(x^2+(y-y'(t))^2)}{\sigma\tilde{w}_0^2}\right], \tag{2}$$

where $\sigma = 1 + (z/z_0)^2$. The Rayleigh range is $z_0 = \pi\tilde{w}_0^2/\lambda$, where λ is the laser wavelength [13].

Our numerical methods are discussed elsewhere [11,14]. Briefly, initial states are found by propagating (1) in imaginary time with $V_{\mathrm{ob}}(\boldsymbol{r},0)$, using a spectral method. Then, real-time simulations are performed subject to motion of the object potential. To recover the essential physics behind the experiment of Raman *et al.* [7], we describe the oscillatory motion by $y'(T) = \alpha - vT$ $(T < 1/2f)$ and $y'(T) = vT - 3\alpha$ $(1/2f < T < 1/f)$, where $T = t - s/f$ and s is the number of completed oscillations. The velocity between the motion extrema is constant, $\boldsymbol{v} = \pm 4\alpha f\hat{\boldsymbol{y}}$, where α is the amplitude and f is the frequency. The condensate is anisotropic, with its long axis along y $(\epsilon < 1)$. As a consequence, for small α, the beam moves though regions of near-constant density. Ini-

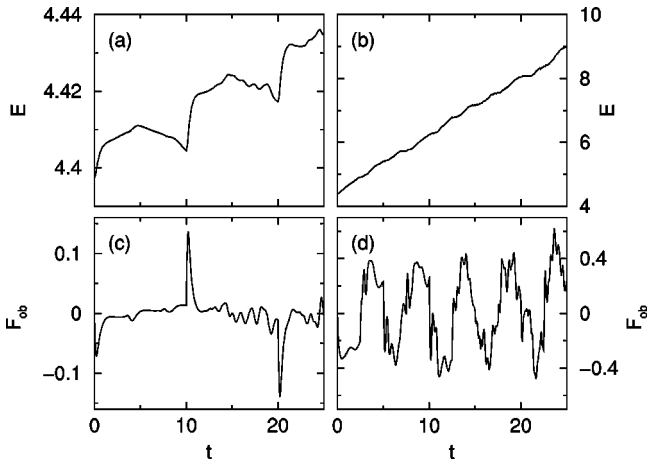

FIG. 1. Time-dependent 2D simulations of laser beam oscillation, with grid spacing of 0.156 (512×128 points) and parameters $C=1000$, $\epsilon=0.0625$, $\alpha=4$, $U_{\rm ob}=20$, and $\tilde{w}_0=1.0$. Condensate energy as a function of time is plotted for (a) $f=0.05$ and (b) $f=0.2$. The drag $F_{\rm ob}$ is also plotted for both frequencies in (c) and (d), respectively.

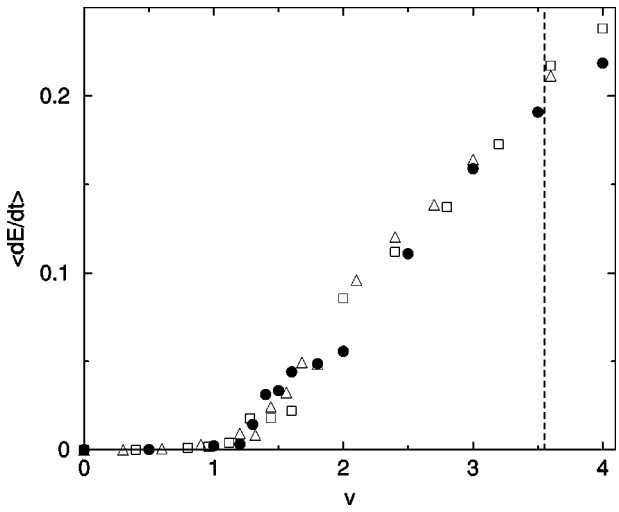

FIG. 2. Mean rate of energy change as a function of velocity for $\alpha=3$ (triangles), $\alpha=4$ (squares), and $\alpha=5$ (bullets). Otherwise, parameters are the same as in Fig. 1. The dashed line shows the speed of sound in the condensate center, $c_s=\sqrt{2\mu}\simeq3.55$. The plot shows a sharp transition between phonon heating (low v) and vortex heating at $v_c\simeq0.4c_s$.

tially, the object creates a density minimum at $y=\alpha$, which follows closely behind the moving object. For $v>v_c$, where $v_c\propto c_s$ and $c_s=\sqrt{2C|\Psi|^2}$ is the sound velocity, the density inside the beam evolves to zero. This is accompanied by a π phase slip [11], at which point the density minimum splits into a pair of vortex lines of equal but opposite circulation [15]. The vortex pair separates, and the process begins again.

The creation of phonons or vortices increases the energy of the condensate, which was calculated numerically using the functional $E=\int(|\nabla\Psi|^2+V|\Psi|^2+C/2|\Psi|^4)d^3r$. The time-independent ground state of the wave function represents the minimum of this functional. The energy is related to the drag force on the object $\boldsymbol{F}_{\rm ob}$ by $dE/dt=\boldsymbol{F}_{\rm ob}\cdot\boldsymbol{v}$. The drag can be calculated independently over the whole condensate using $\boldsymbol{F}_{\rm ob}=-\int|\Psi|^2\boldsymbol{\nabla}V_{\rm ob}d^3r$, allowing a numerical check. Superfluidity corresponds to the situation where E remains constant when $V_{\rm ob}$ is time dependent; i.e., when there is no drag on the object.

Figure 1 shows the energy and drag as a function of time, as calculated for two different frequencies in 2D simulations. At low frequency, the energy transfer is relatively small and characterized by ''jumps'' at the motion extrema, whereas at higher frequency the energy transfer is two orders of magnitude larger and more continuous. Further insight can be gained by considering the drag. At low f, there is little drag except at the motion extrema [Fig. 1(c)], while at high f appreciable drag is observed at all times [Fig. 1(d)].

To measure the average rate of energy transfer, a linear regression analysis is performed on the energy-time data. The gradients are plotted against v in Fig. 2. It can be seen that the curves are characterized by two different regimes. Small energy transfer at low v gives way to enhanced heating above the critical velocity v_c. At high v, the three plots follow a single linear curve.

Energy transfer below v_c arises due to emission of sound waves at the motion extrema. This process (henceforth referred to as phonon heating) is found to approximately scale with v^3, indicating that at each extremum (which are reached at a rate $\propto v$) a sound wave with energy $\sim v^2$ is emitted. Note phonon emission by the object is not inconsistent with Landau's criterion. In particular, the Landau argument relies on the use of Galilean invariance, which breaks down when the condensate density varies, or when the velocity changes abruptly.

For the parameters we have explored, phonon heating is found to be relatively small compared to the energy transfer from vortex formation above v_c. The heating rate in the latter regime is found to scale approximately linearly with v. This implies that the drag force is constant. Indeed, we observe that the drag saturates as v increases. This behavior contrasts with that of steady flow, where the drag $\propto v^k$ (where $k\sim1$ at v close to v_c, and $k\to2$ for $v>c_s$) [8,10]. The difference arises from the oscillatory motion: as the object travels back through its own wake, a large pressure imbalance across the object does not develop.

Figure 3 plots the mean energy transferred against the number of vortex pairs (counted in the simulated wave function). The energy transfer per vortex pair is approximately constant, leading to an estimate of the pair energy, which is plotted as a function of nonlinearity in Fig. 3 (inset). The energy of a vortex pair in an homogeneous condensate with number density n, is given by

$$E_{\rm pair}=\frac{2\pi n\hbar^2}{m}\ln\left(\frac{d}{\xi}\right), \tag{3}$$

where ξ is the healing length and d is the distance between the vortices. Equation (3) is valid for the inhomogeneous condensate when $\xi\ll d\ll R$, where R is the radial extent of the condensate. Equation (3) with $d=2w_0$ is plotted in Fig. 3 (inset), and is found to agree with the numerical data. Recall

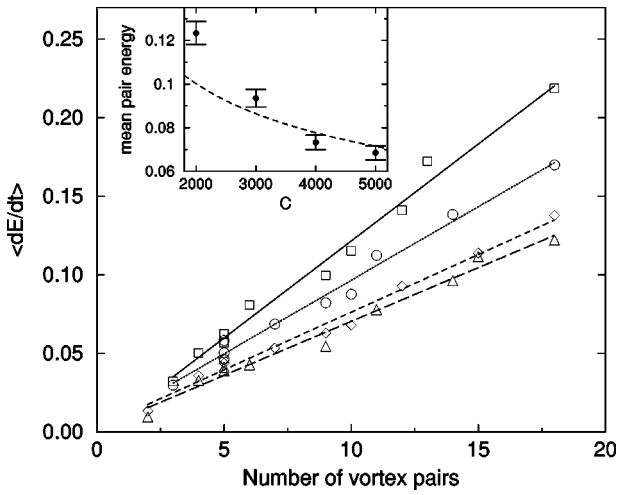

FIG. 3. Number of vortex pairs created up to $t=10$ against rate of energy transfer. Simulation parameters are the same as Fig. 1, with $\alpha=4$ and $C=2000$ (plotted with squares, fit with a solid linear regression line); $C=3000$ (circles, dotted line); $C=4000$ (diamonds, dashed); and $C=5000$ (triangles, long-dashed). The data points closely follow the regression lines, suggesting a constant energy for each vortex pair. Inset: the average pair energy against C, where the dashed line shows the pair energy predicted by Eq. (3).

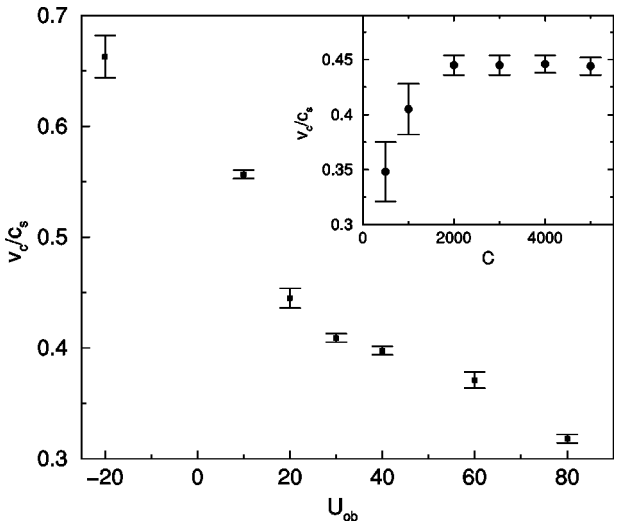

FIG. 4. Critical velocity for vortex formation v_c at $C=2000$ as a function of potential height $U_{\rm ob}$, expressed as a fraction of the speed of sound at the condensate center, c_s. Inset: critical velocity plotted against C, with $U_{\rm ob}=20$. The other parameters in both plots are $\alpha=4$ and $w_0=1$.

that the vortex pair separates immediately after formation, when the pair still resides within the density minimum created by the object. The pair also moves in the direction of the object motion; however, it is slower, and is eventually left behind. At this point, it has an energy approximately equal to $E_{\rm pair}$, and the formation process is complete. The heating rate can be expressed as $dE/dt=E_{\rm pair}\,f_s$ [7], where f_s is the shedding frequency, which is found to be proportional to v. This accounts for the linear dependence of the energy transfer rate.

The subsequent vortex dynamics involve an interplay between velocity fields induced by other vortices and effects arising from the condensate inhomogeneity. In the absence of the object, an isolated pair follows a trajectory similar in character to that of a vortex ring [14], culminating in self-annihilation. However, the object moves back through its wake, interacting with the original pairs and creating more vortices. The circulation of a pair depends upon the direction of the object motion when it is created. So, vortex pairs of opposite circulation are formed and interact when sufficiently close. This leads to situations where vortices annihilate or move towards the edge. The number of vortices remaining within the condensate bulk is found to reach an equilibrium value.

The critical velocity for vortex formation, v_c, as a function of potential height and nonlinear coefficient is shown in Fig. 4. The critical velocity is not as well defined as in the homogeneous case [8–10] for a number of reasons. First, a density inhomogeneity along the direction of motion leads to a variation in c_s, and therefore v_c. However, this is less than $\sim 3\%$ in the simulations considered here. The oscillatory nature of the object motion is important. The time taken for a vortex pair to form diverges to infinity as v approaches v_c from above. So, the measured value of v_c increases from its true value as α decreases. In addition, the object travels through its own low-density wake, where c_s is lower. Vortices can therefore be formed after the first half-oscillation, when v is slightly below v_c. Nevertheless, we can obtain a good estimate for v_c by choosing intermediate values of the amplitude (e.g., $\alpha=4$) and considering only vortex formation during the first half-cycle.

Figure 4 demonstrates that v_c decreases as a function of increasing object potential height, $U_{\rm ob}$, allowing an experi-

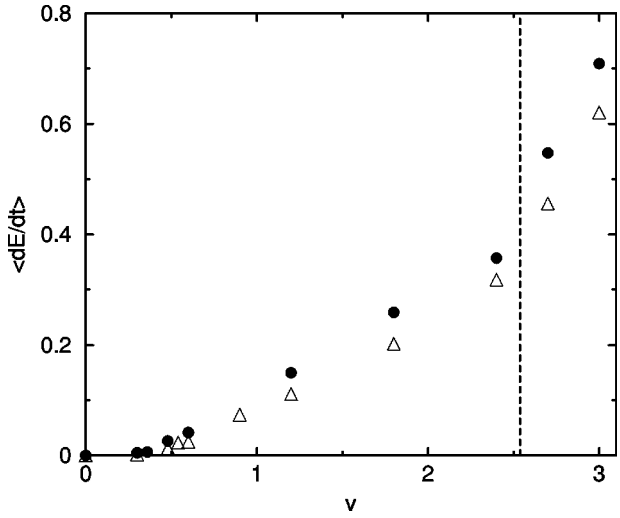

FIG. 5. Mean rate of energy change versus velocity, for 3D simulations with grid spacing 0.234 ($64\times265\times64$ points). Parameters are $C=1000$, $\epsilon=0.0625$, $\eta=1$, $\alpha=3.0$, $\tilde{w}_0=1$, and $\lambda\simeq0.281$. The speed of sound at the condensate center $c_s\simeq2.54$ is represented by the dashed line. For $U_{\rm ob}=40$ (bullets) the critical velocity is $v_c\simeq0.13c_s$, while for $U_{\rm ob}=20$ (triangles) it is $v_c\simeq0.20c_s$.

mental diagnostic for vortex formation at varying beam intensities. This behavior agrees with simulations of 1D soliton creation [16] and vortex ring formation in 3D [17]. We have also studied the case of $U_{\rm ob}<0$, which corresponds to a red-detuned laser. Atoms are attracted to the potential minimum, creating a density peak that moves with the beam. Vortex pairs are created from a density minimum that develops ahead of the beam. Figure 4 (inset) shows v_c as a function of C. The critical velocity tends to a constant value as C increases.

Simulations in 3D were performed, and the mean energy transfer rate as a function of velocity is presented in Fig. 5. Behavior similar to 2D is observed, with smaller critical velocities: a result of the beam intersecting the condensate edge where the speed of sound is lower. Accordingly, vortex lines first appear in these regions and penetrate into the center. This conclusion agrees with the experiment [7,18], where a relatively low critical velocity ($v_c \simeq 0.26 c_s$) was measured. The dependence of v_c on $U_{\rm ob}$ and C was found to be similar to 2D, where, e.g., $v_c \sim 0.29\ c_s$ for $C=4000$ and $U_{\rm ob}=35$. Enhanced heating is also observed for $v_c > c_s$, due to phonon emission between the extrema.

In this paper, we have studied the role of vortex formation in the breakdown of superfluidity, by an oscillating object in a trapped Bose-Einstein condensate. We find that at low object velocities, energy is transferred by phonon emission at the motion extrema, while a much larger energy is transferred above the critical velocity for vortex formation. To generalize these conclusions to realistic experimental situa a tions, the model should include the noncondensed thermal cloud. Energy would then be transferred from the condensed to the thermal cloud by phonon damping [4], or vortex decay [19].

We acknowledge financial support from the EPSRC.

[1] I. M. Khalatnikov, *Introduction to the Theory of Superfluidity* (Addison-Wesley, Redwood City, CA, 1989).

[2] R. P. Feynman, *Progress in Low Temperature Physics* (North-Holland, Amsterdam, 1955), Vol. 1.

[3] W. Ketterle, D. S. Durfee, and D. M. Stamper-Kurn, in *Proceedings of the International School of Physics ''Enrico Fermi'' Course CXL*, edited by M. Inguscio, S. Stringari, and C. Wieman (IOS Press, Amsterdam, 1999); E. A. Cornell, J. R. Enscher, and C. E. Wieman, *ibid*.

[4] F. Dalfovo, S. Giorgini, L. P. Pitaevskii, and S. Stringari, Rev. Mod. Phys. **71**, 463 (1999).

[5] M. R. Matthews, B. P. Anderson, P. C. Haljan, D. S. Hall, C. E. Wieman, and E. A. Cornell, Phys. Rev. Lett. **83**, 2498 (1999).

[6] K. W. Madison, F. Chevy, W. Wohlleben, and J. Dalibard, Phys. Rev. Lett. **84**, 806 (2000).

[7] C. Raman, M. Köhl, R. Onofrio, D. S. Durfee, C. E. Kuklewicz, Z. Hadzibabic, and W. Ketterle, Phys. Rev. Lett. **83**, 2502 (1999).

[8] T. Frisch, Y. Pomeau, and S. Rica, Phys. Rev. Lett. **69**, 1644 (1992).

[9] C. Heupe and M. -É. Brachet, C. R. Acad. Sci., Ser. IIb: Mec., Phys., Chim., Astron. **325**, 195 (1997).

[10] T. Winiecki, J. F. McCann, and C. S. Adams, Phys. Rev. Lett. **82**, 5186 (1999).

[11] B. Jackson, J. F. McCann, and C. S. Adams, Phys. Rev. Lett. **80**, 3903 (1998).

[12] B. M. Caradoc-Davies, R. J. Ballagh, and K. Burnett, Phys. Rev. Lett. **83**, 895 (1999). This work simulated vortex formation when angular momentum is transferred to the condensate by stirring. No dependence of the critical velocity on the speed of sound was found. However, in this case single vortices appear at the edge and are drawn into the bulk by the potential, rather than in [11] where pairs are formed in the object. This suggests that different mechanisms are responsible in each case.

[13] See, e.g., C. S. Adams and E. Riis, Prog. Quantum Electron. **21**, 1 (1997). The potential at the focus is given in h.o.u. by $U_{\rm ob} = -P/(4\pi w_0^2 \Delta \tau^2 I_{\rm sat} \omega_x)$, where τ and $I_{\rm sat}$ are the atomic lifetime and saturation intensity, respectively, while P and Δ are the laser power and detuning.

[14] B. Jackson, J. F. McCann, and C. S. Adams, Phys. Rev. A **61**, 013604 (2000).

[15] Note that, in general, the requirement that vortex pairs are formed ''at a point'' follows from Kelvin's theorem, in order to conserve circulation within an arbitrary closed loop. For infinite potentials [8,10], vortex pairs are nucleated at the surface on opposite sides of the object, so that the circulation within a loop intersecting the surface is not conserved. However, this loop is not closed, as fluid particles cannot enter into the object. Hence, Kelvin's theorem is not violated in this case.

[16] V. Hakim, Phys. Rev. E **55**, 2835 (1997).

[17] T. Winiecki, J. F. McCann, and C. S. Adams, Europhys. Lett. **48**, 475 (1999).

[18] Note that to simulate the experiment [7] directly, the appropriate parameters would be: $\epsilon \simeq 0.077$, $\tilde{w}_0 \simeq 3.5$, $U_{\rm ob} \simeq 220$, and $C \simeq 3.6 \times 10^5$. Such simulations require large grid sizes, making them computationally intensive.

[19] P. O. Fedichev and G. V. Shlyapnikov, Phys. Rev. A **60**, R1779 (1999).